C. R. Geoscience 342 (2010) 600–606

Contents lists available at ScienceDirect

Comptes Rendus Geoscience

www.sciencedirect.com

Internal geophysics

The stress field at Soultz-sous-Forêts from focal mechanisms of induced seismic events: Cases of the wells GPK2 and GPK3

Le champ de contraintes à Soultz-sous-Forêts à partir des mécanismes au foyer des séismes induits : cas des forages GPK2 et GPK3

Louis Dorbath [a,*], Keith Evans [b], Nicolas Cuenot [c], Benoît Valley [b,d], Jean Charléty [e], Michel Frogneux [a]

[a] *EOST, University Louis Pasteur, 5, rue René Descartes, 67084 Strasbourg cedex, France*
[b] *Department of Earth Sciences, Swiss Federal Institute of Technology (ETH), 8092 Zürich, Switzerland*
[c] *GEIE Exploitation minière de la chaleur, 67250 Kutzenhausen, France*
[d] *MIRACO/Laurentian University, Sudbury, Canada*
[e] *GeoscienceAzur, 06560 Sophia Antipolis, France*

ARTICLE INFO

Article history:
Received 8 January 2009
Accepted after revision 8 December 2009
Available online 18 February 2010

Written on invitation of the Editorial Board

Keywords:
Soultz-sous-Forêts
Focal mechanisms
Stress field
France

ABSTRACT

The stress field at the EGS geothermal site of Soultz-sous-Forêts has been the subject of many studies, because it largely controls the response of the reservoir to fluid injection. The analysis of borehole logging data, especially breakouts and drilling-induced tension fractures, in the four geothermal wells define an average SHmax orientation ranging between 170° and 180° down to 5 km depth. It also reveals strong heterogeneities in several depth intervals. In this paper, the inversion of double-couple source mechanisms of seismic events induced during GPK2 and GPK3 stimulation tests is performed to retrieve the orientation and shape factor of the stress tensor, using the *Slickenside Analysis Package* of Michael (1984, 1987a, 1987b). The results indicate a well-determined orientation of Shmin in GPK2 and in GPK3; in GPK3 Shmin is clockwise rotated by about 10°. The stress tensor defines an uniaxial extension. The results from both methods, analysis of borehole logging data and inversion of focal mechanisms, are only slightly different; the discrepancy may be due to the larger reservoir volume covered by the focal mechanisms, which can include strong stress heterogeneities.

© 2010 Académie des sciences. Published by Elsevier Masson SAS. All rights reserved.

Mots clés :
Soultz-sous-Forêts
Mécanismes au foyer
Contraintes
France

RÉSUMÉ

Le champ de contraintes à Soultz-sous-Forêts, où est installé le projet EGS de Géothermie, a fait l'objet de nombreuses études, étant donné son importance dans la réponse du réservoir aux stimulations hydrauliques. L'analyse des données de diagraphie dans les puits, principalement les fractures induites durant le forage, permettent de fixer la direction de SHmax entre 170° et 180° dans le granite. Dans cet article, l'inversion des mécanismes au foyer (double-couple) des microséismes induits au cours des stimulations de GPK2 et GPK3 est réalisée à l'aide du *Slickenside Analysis Package* de Michael (1984, 1987a, 1987b), afin de déterminer l'orientation et le facteur de forme du tenseur des contraintes. L'inversion montre que la direction de Shmin est bien établie dans GPK2 et

* Corresponding author.
E-mail addresses: louis.dorbath@eost.u-strasbg.fr, louis.dorbath@unistra.fr (L. Dorbath).

1631-0713/$ – see front matter © 2010 Académie des sciences. Published by Elsevier Masson SAS. All rights reserved.
doi:10.1016/j.crte.2009.12.003

GPK3. On observe une rotation horaire de 10° de cette direction de GPK2 à GPK3. Le tenseur définit une extension uniaxiale. Les résultats des deux méthodes, analyse des données de diagraphie et inversion des mécanismes au foyer, sont proches, les différences proviennent probablement du fait que le volume échantillonné par les mécanismes focaux est plus grand et inclut des hétérogénéités de contrainte.

© 2010 Académie des sciences. Publié par Elsevier Masson SAS. Tous droits réservés.

1. Introduction

The study of the stress field at the geothermal site of Soultz-sous-Forêts (Alsace, France) is a story as long as the project itself. This fact underlines the importance of knowledge of the stress field for the development of deep geothermal projects. The stress field and the orientation of the pre-existing fractures and faults are two key parameters which together largely define the response of the medium to massive fluid injections. The stress field at Soultz has thus been the subject of many studies and there is a substantial literature on the subject. The first studies were carried out after the drilling of the first borehole GPK1 to 2000 m in 1987 (Jung, 1991; Rummel and Baumgärtner, 1991), and continued with the extension of this well to about 3500 m depth. Until recently, the characterization of the stress field in the deeper reservoir at 5000 m depth was largely based on the extrapolation of the results from the shallow reservoir (Cornet et al., 2007; Klee and Rummel, 1999). In the last few of years, however, the data from the deep reservoir have placed direct constraints on the stress state (Valley and Evans, 2007b).

The orientation and magnitude of the principal stresses can be constrained through the study of breakouts and drilling-induced tension fractures (DITFs) that are seen in all deep wells, augmented by hydraulic data from large injections or small-volume dedicated stress tests. Another insight into the stress field can be obtained by examining the focal mechanisms of the seismic events induced by the injections. However, in this case, only the deviatoric part of the stress tensor can be determined, the absolute values of the principal stresses being strictly undetermined. Nevertheless, the stress magnitudes can be calculated if we assume that the vertical principal stress corresponds to the lithostatic load. Results obtained with this method differ sometimes from the direct observation of breakouts and DITFs. For instance, Helm, 1996 proposed a value of $124^\circ \pm 20^\circ$ for the orientation of the maximum horizontal principal stress,[1] SHmax, from an analysis of microseismic events induced during the stimulation of the 3.0–3.5 km reservoir, whereas studies of breakouts and DITFs of boreholes in this reservoir provide an extraordinarily well-defined indication that SHmax above 3.8 km is on average oriented $N175^\circ \pm 10^\circ$ (Cornet et al., 2007). The discrepancy can be partly explained by the uncertainty on the determination of the fault plane and the auxiliary plane of the focal mechanisms, which were not very well constrained, as recognized by Helm, 1996. The recent studies of stress in the deeper reservoir by Valley and Evans, 2007a, as well as a better determination of focal mechanisms of events induced during its stimulation, due to the installation of numerous seismic stations during the stimulation of GPK2 and GPK3 (Dorbath et al., 2009), allow us to re-address the issue of the characterization of the deep stress field. This is the purpose of the present article.

2. Stress orientation and magnitude from borehole observations

As early as 1988, Mastin and Heinemann, 1998 analysed the data from 4-arm caliper and ultrasonic televiewer (BHTV) logs in GPK1 and concluded that the direction of the maximum horizontal principal stress, SHmax was $N169^\circ \pm 21^\circ$. Rummel and Baumgärtner, 1991 applied the HTPF stress determination technique to just five hydraulic tests performed between 1458 and 1989 m depth in GPK1 and found SHmax was oriented $N155^\circ \pm 3^\circ$. However, given the few number of data, this cannot be considered a reliable estimate (Cornet et al., 2007). Tenzer et al., 1992 analysed breakouts and DITFs for the same depth range in the same well and found an SHmax orientation of $N169^\circ \pm 11^\circ$. Nagel, 1994 analyzed vertical DITFs in GPK1 after its extension to 3600 m and found an SHmax orientation of $181^\circ \pm 22^\circ$. Brudy and Zoback, 1999 extended Nagel's study by adding *en échelon* DITFs and found the same SHmax orientation. Hydrofracture stress tests performed in 1993 between 2195 and 3506 m as reported by Klee and Rummel, 1993 provide stress magnitude but no orientation information. Heinemann-Glutsch, 1994 analysed all stress data collected up to 1993 and proposed linear variations of stress magnitude with depth and an SHmax orientation of N170°E. Bérard and Cornet, 2003 identified breakouts in GPK1 between 2850 m and 3465 m and indicated an SHmax orientation of $N5^\circ E \pm 7^\circ$. Genter and Tenzer, 1995 identified vertical DITFs in GPK2 in the depth range 1420–3880 m and reported SHmax orientation of $N175^\circ \pm 17^\circ$.

Stress orientation in the deeper reservoir as revealed by breakouts and DITFs in the two 5 km deep wells, GPK3 and GPK4, was studied by Valley and Evans, 2005; Valley and Evans, 2007a. DITFs dominate above 3 km whereas breakouts dominate below 3.5 km. Axial DITFs in GPK3 above 3257 m MD[2] depth indicate a mean SHmax direction of $N167^\circ \pm 12^\circ$. Below 3257 m MD in GPK3, the numerous breakouts indicate an SHmax orientation of $N162^\circ \pm 20^\circ$. The large standard deviation is partly due to the presence of a

[1] Throughout this paper, SHmax represents the maximum horizontal principal stress, Shmin the minimum horizontal principal stress, and Sv the vertical stress.

[2] This denotes measured depth along borehole and is not the same true vertical depth since GPK3 and GPK4 are inclined.

fault that cuts the borehole at 4770 m MD (Hettkamp et al., 2004), and perturbs the stress orientation by up to 90° over several hundred meters (Valley and Evans, 2007b). In GPK4, the DITFs in the upper part of the well indicate an SHmax orientation of N172° ± 12°. Below 3.7 km MD, the breakouts are numerous and show two large-scale systematic changes in orientation associated with fracture zones. They suggest that the mean SHmax orientation over the lowermost 1.5 km of hole is N174° ± 17°.

Maximum pressures at the casing shoes during the stimulation of the three deep wells appeared to be limited by jacking (Valley and Evans, 2007a), and lay on the Shmin magnitude trend proposed by Cornet et al., 2007. The profiles of the presence or absence of breakouts and DITFs along the wells GPK3 and GPK4 suggest SHmax lies between 0.9 and 1.05 times the value of the vertical principal stress Sv (Valley and Evans, 2007a), indicating a quasi uniaxial extensive stress regime.

3. Stress orientation from focal mechanisms

We used the seismological data recorded during the 2000 and 2003 hydraulic stimulations of the lower reservoir in GPK2 and GPK3 respectively to estimate the stress field about the lower sections of these holes. The study used 100 well-constrained focal mechanisms from the six days long injection stimulation of GPK2, from 30th June to 5th July 2000 (Weidler, 2000), and 96 from the 10 days long injection stimulation of GPK3, from 27th May to 7th June 2003 (Baria et al., 2004; Hettkamp et al., 2004). All of these are compatible with a double couple model of slip. No evidence for tensile rupture within the geothermal reservoir has been noticed, which means that the tensile component is weak or non-existent. This is in agreement with the purpose of the stimulation, that is large water injections induce shearing on pre-existing fractures favourably oriented in the regional stress field since the increasing pore fluid pressure is likely to reduce the effective normal stress on the fractures. The determination of seismic moment tensor for induced seismic events in GPK3 results in the absence of any NDC (non double couple) component in the source mechanisms (Horálek et al., 2008).

The GPK2 events all occurred during the first two days of the injection, whereas the GPK3 events occurred throughout the injection. Consequently, hypocenters of the GPK2 events tend to be located near the injection whereas those from GPK3 spread over a larger volume. The seismological data recorded during the 2004 and 2005 stimulation injections of GPK4, the third 5 km deep well at Soultz, do not allow sufficiently well-constrained focal mechanisms to be derived. Thus we restrict the analysis to the GPK2 and GPK3 data. The focal mechanism solutions (FMSs) for GPK2 are constrained by at least 12 P-wave first-motion polarities recorded on both surface and downhole instruments, and the GPK3 events with at least 15. The FMSs are determined automatically with the code FPFIT (Reasenberg and Oppenheimer, 1985) and fine-tuned by hand without any wrong polarity. The azimuthal coverage is usually good, so that there are always at least three covered quadrants and there is no need to use the S-wave to constrain the focal planes (see Cuenot et al., 2006), for more details on the seismic array deployed at Soutz-sous-Forêts during the stimulation tests. The location of the microearthquakes used in this study has been obtained through a local tomography method which allows to determine the 3-D velocity model together with the hypocenters coordinates (Charléty et al., 2006; Cuenot et al., 2008). The uncertainties have been estimated to 50 m and 70 m on the horizontal and vertical position respectively. The uncertainties on the azimuth and dip of the planes (or, at least, one of them) are around 10°.

We inverted the focal mechanism solutions for stress using the *Slickenside Analysis Package* of Michael, 1984; Michael, 1987a; Michael, 1987b. Initially, for each injection, the full collection of FMSs was inverted with *a priori* fixed fault planes. The results showed that the discrepancies between the 'observed' and predicted slip vectors in the fault plane, the misfit, for several mechanisms were unacceptably large, sometimes greater than 50°. Thus, for the next inversion run, the fault and auxiliary planes were switched for mechanisms that had a misfit greater than 30°. In many cases, the misfit decreased significantly, and so the new planes were retained. However, in some cases the misfit remained large. These events were thus excluded from the calculation. The process was then repeated with the maximum misfit angle reduced by 5°, and so on until the maximum misfit angle reached 10°, which is comparable to the uncertainty in the 'observed' slip angle. At the end of this process, we obtained a stress tensor and a set of mechanisms which are compatible. We also checked that the misfit of the mechanisms which were excluded in the process remained large. For GPK2, 66 mechanisms out of 100 were found to have a misfit less than 10°, and 21 mechanisms showed a misfit higher than 15°. For GPK3, the numbers are 62 and 23, respectively. As suggested by Michael, 1987a; Michael, 1987b, we bootstrap resample the data set 1000 times flipping the selected fault and slip direction 10% of the time. As the fault planes were selected in the previous step, the resampling is only performed on the fault planes. We thus calculated 1000 stress tensors for each set of mechanisms. The principal directions of the tensors are presented in Fig. 1a (GPK2) and 2a (GPK3). On the same figures are shown the focal mechanisms used for the inversion (1b, 1c and 1d for GPK2; 2b, 2c and 2d for GPK3).

The principal directions of the stress tensor are reasonably well-determined for GPK2. σ_3, which is Shmin, is well constrained, and is near-horizontal with an orientation of N68° ± 5°. Inverting the whole data set of 100 events yields an average Shmin direction of N68.3°, whereas for the 79 events with a misfit threshold less than 15°, the orientation is N69.9°. The vast majority of solutions for $\sigma 1$ cluster near vertical, consistent with the predominant normal faulting component in the FMSs. The deviation of this axis from true verticality might be ascribed to local stress heterogeneity whose existence is demonstrated by the variations in orientation of breakouts and DITFs on scales of a hundred metres or more (Valley and Evans, 2007b). Alternatively, it might be due to near-equivalence of the magnitudes of $\sigma 1$ and $\sigma 2$, implying a uniaxial extensional stress state, which would also explain the scattering of a few

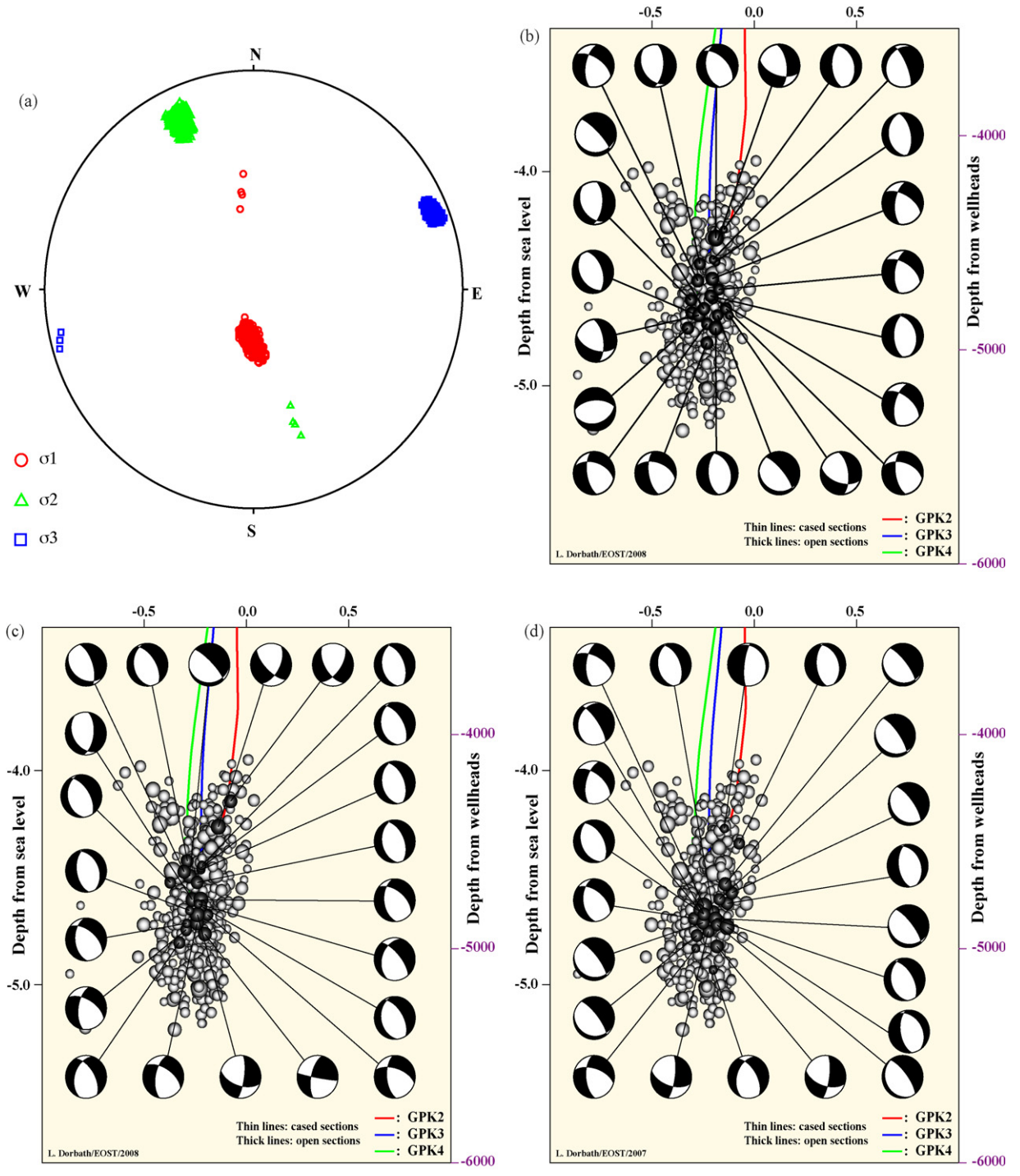

Fig. 1. GPK2: a: Principal stress directions; b, c and d: focal mechanisms used in the inversion of the stress tensor. Light grey: hypocenters of $M > 1$ microearthquakes induced by GPK2 stimulation (June/July 2000). Black: hypocenters of microearthquakes used in the inversion.

Fig. 1. GPK2 : a : Principales directions de contrainte ; b, c et d : mécanismes focaux utilisés dans l'inversion du tenseur de contrainte. Gris clair : hypocentres des microséismes $M > 1$, induits par simulation GPK2 (juin/juillet 2000). Noir : hypocentres des microséismes utilisés dans l'inversion.

inclined solutions across the plane normal to σ3. However, the shape factor *F*, defined as (σ2-σ3)/(σ1-σ3) is ∼0.75, rather than the value of 1.0 that would define a uniaxial extensional regime. Normal faulting is dominant among the focal mechanism solutions. If we consider the west-dipping plane as the fault plane (even if it is actually not), then an azimuth for this plane of around 140°/150° would imply the shear component is dextral, while it would be senestral for azimuths of the order of 170°/180°. This is completely in agreement with the direction of extension. On Fig. 1c and d,

we can notice strike-slip mechanisms with a normal component on N120° faults.

The distribution of principal axis orientations for the GPK3 data (Fig. 2a) also shows that σ3 (i.e. Shmin) is well constrained to be horizontal, but is oriented at N77° ± 4°. The solutions for the other two principal stress axes form a continuous band across the stereoplot, indicating the stress state has cylindrical symmetry consistent with a uniaxial extension regime. The shape factor value of ~0.9 estimated for the shape factor with the 62 events data set is reasonably

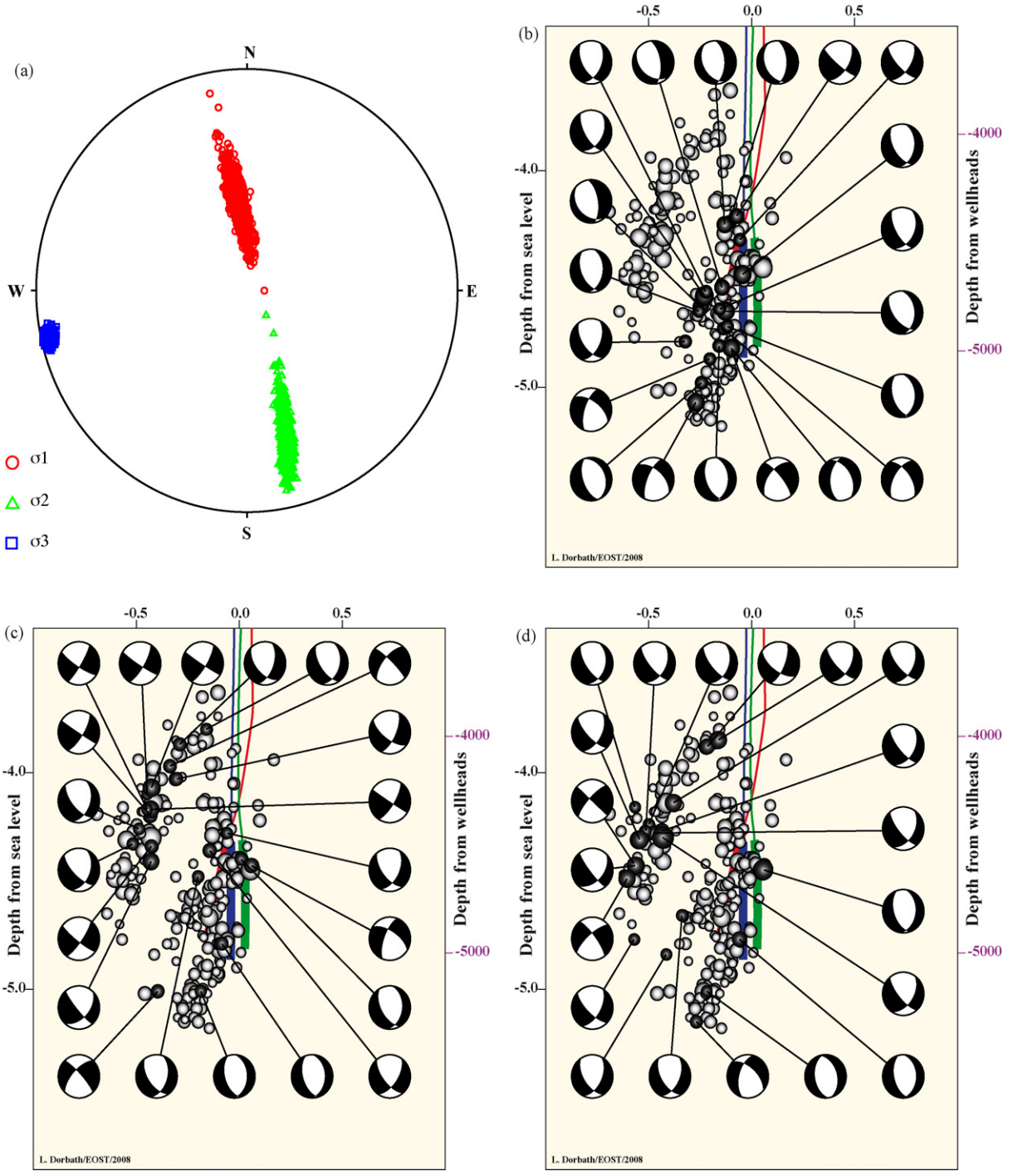

Fig. 2. a, b, c, d: same as Fig. 1 for GPK3. Light grey: hypocenters of $M > 1$ microearthquakes induced by GPK3 stimulation (May/June 2003). Black: hypocenters of microearthquakes used in the inversion.

Fig. 2. a, b, c, d : identique à la Fig. 1 pour GPK3. Gris clair : hypocentres des microséismes $M > 1$, induits par simulation GPK3 (mai/juin 2003). Noir : hypocentres des microséismes, utilisés dans l'inversion.

consistent with uniaxial extension. The mechanisms (Fig. 2 b–d) are more or less very similar to those observed in GPK2. Nevertheless, close scrutiny reveals that the dextral strike-slip movements occur on planes whose strike is larger than in the GPK2 examples. This would be consistent with a slight rotation in the orientation of σ3. We also observe more mechanisms with a dominant strike-slip feature.

4. Discussion

4.1. GPK2

As noted earlier, the state of stress in the shallow reservoir above 3.8 km is well established through studies of hydraulic tests and wellbore failure in wells GPK1 and GPK2. These have provided a very well-constrained estimate of the orientation of SHmax of N175° ± 10°. In the deeper reservoir, wellbore failure observations have been analysed in wells GPK3 and GPK4 to provide estimates of SHmax orientation. However, no reliable estimates are available for the deeper part of GPK2 owing to poor quality BHTV data. In the section of GPK2 above 3.8 km, Genter and Tenzer, 1995 found an orientation of N175° for SHmax based upon DITFs, which represents a difference of 15° with the SHmax orientation of N160° obtained from the inversion of focal mechanisms of events occurring in the rock mass about the lower section of the well. Valley and Evans, 2007a found an average SHmax orientation for GPK3 and GPK4 in the lower reservoir of N168° ± 19°, which is approximately midway between the two.

Cuenot et al., 2006 inverted the first-motion polarities of subsets of events induced by the 2000 GPK2 stimulation in the deep reservoir using the inversion procedure of Rivera and Cisternas, 1990. For the inversion of a subset of events that lay near the upper part of the reservoir, they obtained an undetermined result, where only σ1 was well-constrained and vertical. However, inversion of a subset that lay in the lower part of the reservoir yielded a well-determined Shmin-orientation of N244° (i.e. N64°) ± 20°, with the other two principal axes forming an unconstrained band across the stereoplot. The Shmin-orientation is similar to the N70° obtained with the present inversion, but with much higher uncertainties. The higher error is due to the fact that Cuenot et al., 2006 did not remove poorly-fitting events from the inversion, as was done in the present study.

4.2. GPK3

In comparison to the stress tensor calculated with GPK2 data, the tensor determined in GPK3 presents two significant changes. Firstly, there is an apparent anticlockwise rotation of σ3 of about 10°: from N68° ± 5° for GPK2 to N77° ± 4° for GPK3. Secondly, a symmetry of rotation around σ3 is observed, indicating very similar values for σ1 and σ2.

In the lower part of GPK3, Valley and Evans, 2007a found an Shmin orientation of N71° ± 20° from breakouts, which is consistent with the inversion results for both GPK2 and GPK3, the standard deviation being too large to discriminate. The large standard deviation is due in large part to a large-scale disturbance of the stress field extending

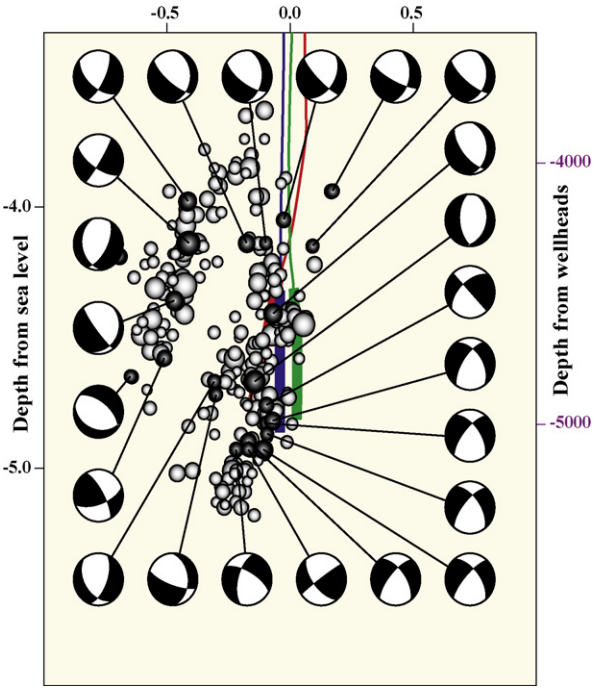

Fig. 3. Black: focal mechanisms with large (> 15°) misfit. Light grey: hypocenters of $M > 1$ microearthquakes induced by GPK3 stimulation (May/June 2003).

Fig. 3. Noir : mécanismes focaux avec grandes imperfections (> 15°). Gris clair : hypocentres des microséismes $M > 1$, induits par simulation GPK3 (mai/juin 2003).

along the GPK3 well between 4.5 and 4.8 km (true vertical depth) that is associated with a fault that dips at 50–60° towards N250° (Valley and Evans, 2007b). This perturbation results in changes in Shmin-orientation of up to 90°. The presence of such large perturbation is the principal justification for the process of removing focal mechanism solutions from the inversion that high large misfit since these are likely to be occurring within a stress perturbation. On Fig. 3, we show the location of the 23 seismic events for which the misfit between the observed and the calculated slip direction is higher than 15°. It can be seen that 11 of the 23 focal mechanisms are clustered within the cloud close to GPK3 (on this projection view) at depths between 4800 m and 5100 m.

5. Conclusion

In conclusion, direct observation of breakouts and DITFs in the boreholes appears to be the most accurate method to determine the linear-with-depth state of stress, and quantify the deviations from this (i.e. the heterogeneity). Nevertheless the inversion of focal mechanisms can yield useful characteristics of the stress field, and has the advantage that it samples a much larger volume. The results obtained in the present study show that, for the well-constrained stresses, the discrepancy between the results of the focal mechanism and the wellbore failure observations is less than the uncertainty range. The approach of selecting compatible mechanisms produces simultaneously a set of rejected mechanisms, which can, in

some favourable cases, highlight zones of strong stress heterogeneities.

Acknowledgements

Work at Soultz is funded and supported by the European Commission Directorate-General Research, contract SE6-CT-2003-502 706, EGS Pilot Plant, ADEME (contract ADEME-CNRS No. 05.05.C0076), the German Bundesministerium für Umwelt, Naturschutz und Reakorsicherheit, the Projektträger of the Forshungszentrtrum Jülich in Germany and the members of the GEIE "Exploitation Minière de la Chaleur" (EDF, EnBW, ES, Pfalzwerke, Evonik). The research was conducted with the financial support of ADEME. K. Evans and B. Valley acknowledge the support of the Swiss State Secretariat for Education and Science.

References

Baria, R., Michelet, S., Baumgärtner, J., Dyer, B., Gérard, A., Nicholls, J., Hettkamp, T., Deza, D., Soma, N., Asanuma, H., Garnish, J., Megel, T., 2004. Microseismic monitoring of the world's largest potential HDR reservoir. In: Proceedings 29th Workshop on Geothermal Reservoir Engineering, Standford University, Standford, California, 26/28th January, p. 8.

Bérard, T., Cornet, F.H., 2003. Evidence of thermally induced borehole elongation: a case study at Soultz, France. Int. J. Rock Mech. Min. Sci. 40, 1121–1140.

Brudy, M., Zoback, M.D., 1999. Drilling-induced tensile wall-fractures: implications for determination of in-situ stress orientation and magnitude. Int. J. Rock Mech. Min. Sci. 36 (1999), 191–215.

Charléty, J., Cuenot, N., Dorbath, C., Dorbath, L., 2006. Tomographic study of the seismic velocity at the Soultz-sous-Forêts EGS/HDR site. Geothermics 35, 532–543.

Cornet, F.H., Bérard, T., Bourouis, S., 2007. How close to failure is a granite rock mass at a 5 km depth? Int. J. Rock. Mech. Min. Sci. 44, 47–66.

Cuenot, N., Charléty, J., Dorbath, L., Haessler, H., 2006. Faulting mechanisms and stress regime at the European HDR site of Soutz-sous-Forêts, France. Geothermics 35, 561–575.

Cuenot, N., Dorbath, C., Dorbath, L., 2008. Analysis of the Microseismicity Induced by Fluid Injections at the Hot Dry Rock site of Soultz-sous-Forêts (Alsace, France): Implications for the Characterization of the Geothermal Reservoir Properties. Pure Appl. Geophys. 165, 797–828.

Dorbath, L., Cuenot N., Genter A., Frogneux M., 2009. Seismic response of the fractured and faulted granite of Soultz-sous-Forêts (France) to 5 km deep massive water injections, Geophys. J. Int. 177, 653–675.

Genter, A., Tenzer, H., 1995. Geological monitoring of GPK-2 HDR borehole, 1420-3880 m. BRGM, Orléans.

Heinemann-Glutsch, B., 1994. Results of scientific investigations at the HDR test site, Soultz-sous-Forêts, Alsace, Socomine, BP 38, route de Soultz, 67250 Kutzenhausen, France.

Helm, J.A., 1996. The natural seismic hazard and induced seismicity of the European HDR (Hot Dry Rock) geothermal energy project at Soultz-sous-Forêts, France. Ph.D. thesis, université Louis-Pasteur de Strasbourg.

Hettkamp, T., Baumgärtner, J., Baria, R., Gérard, A., Gandy, T., Michelet, S., Teza, D., 2004. Electricity production from Hot Rocks. In: Proceedings 29th Workshop on Geothermal Reservoir Engineering, Stanford University, Stanford, California, 26/28th January, p. 10.

Horálek, J., Jechumtálová, Z., Dorbath, L., Šilený, J., 2008. Shear vs. non-shear components in source mechanisms of micro-earthquakes induced in hydraulic fracturing experiment in the HDR site of Soultz-sous-Forêts (Alsace) in 2003. In: Proceedings of the EHDRA Scientific meeting, Soultz-sous-Forêts, 24/25 September, p. 9.

Jung, R., 1991. Hydraulic fracturing and hydraulic testing in the granitic section of borehole GPK1, Soulz-sous-Forêts. Geothermal Sci. Tech. 3, 149–198.

Klee, G., Rummel, F., 1993. Hydrofrac stress data for the European HDR research project test site Soultz-sous-Forêts. Int. J. Rock Mech. Min. Sci. Geomech. Abst. 30, 973–976.

Klee, G., Rummel, F., 1999. Stress regime in the Rhinegraben basement and in the surrounding tectonic units. In: Lang, P. (Ed.), Proceedings of the European Geothermal Conference, 28/29/30th September, Bull. Hydrogéologie Special Issue 135–142, Bern, Switzerland.

Mastin, L., Heinemann, B., 1998. Evaluation of the caliper and televiewer data fromm the Soultz well between 1450 m and 2000 m depth. Karlsruhe University, Germany.

Michael, A.J., 1984. Determination of stress from slip data: faults and folds. J. Geophys. Res. 89 11 517-11 526.

Michael, A.J., 1987a. The use of focal mechanisms to determine stress: a control study. J. Geophys. Res. 92, 357–368.

Michael, A.J., 1987b. Stress rotation during the Coalinga aftershock sequence. J. Geophys. Res. 92 (7), 963–7979.

Nagel, R, 1994. Das Spannungsfeld in der Geothermiebohrung Soultz-sous-Forêts abgeleitet aus vertikalen Structuren in eine Tiefe von 1.9 bis 3.6 km, PhD thesis, Univ. Karlsruhe.

Reasenberg, P.A., Oppenheimer, D., 1985. FPFIT, FPPLOT and FPPAGE: Fortran computer programs for calculating and displaying earthquake fault-plane solutions. US Geolog. Survey 25.

Rivera, L., Cisternas, A., 1990. Stress tensor and fault plane solutions for a population of earthquakes. Bull. Seismol. Soc. Am. 80, 600–614.

Rummel, F., Baumgärtner, J., 1991. Hydraulic fracturing stress measurements in the GPK1 borehole, Soultz-sous-Forêts. Geotherm. Sci. Tech. 3, 119–148.

Tenzer, H., Mastin, L., Heinemann, B., 1992. Determination of planar discontinuities and borehole geometry in the crystalline rock of borehole GPK-1 at Soulz-sous-Forêts. Geothermal Sci. Tech. 3, 31–68.

Valley, B., Evans, K.F., 2005. Stress orientation estimates from analysis of breakouts and drilling-induced tension fractures in GPK3 and GPK4. In: Proceedings EHDRA Scientific Conference, Soultz-sous-Forêts, 17/18th March.

Valley, B., Evans, K.F., 2007a. Stress state at Soultz-sous-Forêts to 5 km depth from wellbore failure and hydraulic observations. In: Proceedings 32nd Workshop on Geothermal Reservoir Engineering, Stanford University, Stanford, California, 22–24th January, p. 10.

Valley, B., Evans, K.F., 2007b. Stress heterogeneity in the Soultz granite inferred from analysis of wellbore failure to 5 km depth. In: Proceedings EHDRA Scientific Conference, Soultz-sous-Forêts. 28–29th June, p. 10.

Weidler R., 2000. Hydraulic stimulation of the 5 km deep well GPK-2, Report to Socomine, Bundesanstalt für Geowissenschaften und Rohstoffe (BGR) Hannover.